

Elliptic Flow for ϕ Mesons and (Anti)deuterons in Au + Au Collisions at $\sqrt{s_{NN}} = 200$ GeV

S. Afanasiev,¹⁷ C. Aidala,⁷ N. N. Ajitanand,⁴³ Y. Akiba,^{37,38} J. Alexander,⁴³ A. Al-Jamel,³³ K. Aoki,^{23,37} L. Aphecetche,⁴⁵ R. Armendariz,³³ S. H. Aronson,³ R. Auerbeck,⁴⁴ T. C. Awes,³⁴ B. Azmoun,³ V. Babintsev,¹⁴ A. Baldisseri,⁸ K. N. Barish,⁴ P. D. Barnes,²⁶ B. Bassalleck,³² S. Bathe,⁴ S. Batsouli,⁷ V. Baublis,³⁶ F. Bauer,⁴ A. Bazilevsky,³ S. Belikov,^{3,16} R. Bennett,⁴⁴ Y. Berdnikov,⁴⁰ M. T. Bjornedal,⁷ J. G. Boissevain,²⁶ H. Borel,⁸ K. Boyle,⁴⁴ M. L. Brooks,²⁶ D. S. Brown,³³ D. Bucher,²⁹ H. Buesching,³ V. Bumazhnov,¹⁴ G. Bunce,^{3,38} J. M. Burward-Hoy,²⁶ S. Butsyk,⁴⁴ S. Campbell,⁴⁴ J.-S. Chai,¹⁸ S. Chernichenko,¹⁴ J. Chiba,¹⁹ C. Y. Chi,⁷ M. Chiu,⁷ I. J. Choi,⁵² T. Chujo,⁴⁹ V. Cianciolo,³⁴ C. R. Cleven,¹² Y. Cobigo,⁸ B. A. Cole,⁷ M. P. Comets,³⁵ P. Constantin,¹⁶ M. Csanád,¹⁰ T. Csörgő,²⁰ T. Dahms,⁴⁴ K. Das,¹¹ G. David,³ H. Delagrange,⁴⁵ A. Denisov,¹⁴ D. d'Enterria,⁷ A. Deshpande,^{38,44} E. J. Desmond,³ O. Dietzsch,⁴¹ A. Dion,⁴⁴ J. L. Drachenberg,¹ O. Drapier,²⁴ A. Drees,⁴⁴ A. K. Dubey,⁵¹ A. Durum,¹⁴ V. Dzhordzhadze,⁴⁶ Y. V. Efremenko,³⁴ J. Egdemir,⁴⁴ A. Enokizono,¹³ H. En'yo,^{37,38} B. Espagnon,³⁵ S. Esumi,⁴⁸ D. E. Fields,^{32,38} F. Fleuret,²⁴ S. L. Fokin,²² B. Forestier,²⁷ Z. Fraenkel,⁵¹ J. E. Frantz,⁷ A. Franz,³ A. D. Frawley,¹¹ Y. Fukao,^{23,37} S.-Y. Fung,⁴ S. Gadrat,²⁷ F. Gastineau,⁴⁵ M. Germain,⁴⁵ A. Glenn,⁴⁶ M. Gonin,²⁴ J. Gosset,⁸ Y. Goto,^{37,38} R. Granier de Cassagnac,²⁴ N. Grau,¹⁶ S. V. Greene,⁴⁹ M. Grosse Perdekamp,^{15,38} T. Gunji,⁵ H.-Å. Gustafsson,²⁸ T. Hachiya,^{13,37} A. Hadj Henni,⁴⁵ J. S. Haggerty,³ M. N. Hagiwara,¹ H. Hamagaki,⁵ H. Harada,¹³ E. P. Hartouni,²⁵ K. Haruna,¹³ M. Harvey,³ E. Haslum,²⁸ K. Hasuko,³⁷ R. Hayano,⁵ M. Heffner,²⁵ T. K. Hemmick,⁴⁴ J. M. Heuser,³⁷ X. He,¹² H. Hiejima,¹⁵ J. C. Hill,¹⁶ R. Hobbs,³² M. Holmes,⁴⁹ W. Holzmann,⁴³ K. Homma,¹³ B. Hong,²¹ T. Horaguchi,^{37,47} M. G. Hur,¹⁸ T. Ichihara,^{37,38} K. Imai,^{23,37} M. Inaba,⁴⁸ D. Isenhower,¹ L. Isenhower,¹ M. Ishihara,³⁷ T. Isobe,⁵ M. Issah,⁴³ A. Isupov,¹⁷ B. V. Jacak,^{44,*} J. Jia,⁷ J. Jin,⁷ O. Jinnouchi,³⁸ B. M. Johnson,³ K. S. Joo,³⁰ D. Jouan,³⁵ F. Kajihara,^{5,37} S. Kametani,^{5,50} N. Kamihara,^{37,47} M. Kaneta,³⁸ J. H. Kang,⁵² T. Kawagishi,⁴⁸ A. V. Kazantsev,²² S. Kelly,⁶ A. Khanzadeev,³⁶ D. J. Kim,⁵² E. Kim,⁴² Y.-S. Kim,¹⁸ E. Kinney,⁶ A. Kiss,¹⁰ E. Kistenev,³ A. Kiyomichi,³⁷ C. Klein-Boesing,²⁹ L. Kochenda,³⁶ V. Kochetkov,¹⁴ B. Komkov,³⁶ M. Konno,⁴⁸ D. Kotchetkov,⁴ A. Kozlov,⁵¹ P. J. Kroon,³ G. J. Kunde,²⁶ N. Kurihara,⁵ K. Kurita,^{39,37} M. J. Kweon,²¹ Y. Kwon,⁵² G. S. Kyle,³³ R. Lacey,⁴³ J. G. Lajoie,¹⁶ A. Lebedev,¹⁶ Y. Le Bornec,³⁵ S. Leckey,⁴⁴ D. M. Lee,²⁶ M. K. Lee,⁵² M. J. Leitch,²⁶ M. A. L. Leite,⁴¹ H. Lim,⁴² A. Litvinenko,¹⁷ M. X. Liu,²⁶ X. H. Li,⁴ C. F. Maguire,⁴⁹ Y. I. Makdisi,³ A. Malakhov,¹⁷ M. D. Malik,³² V. I. Manko,²² H. Masui,⁴⁸ F. Matathias,⁴⁴ M. C. McCain,¹⁵ P. L. McGaughey,²⁶ Y. Miake,⁴⁸ T. E. Miller,⁴⁹ A. Milov,⁴⁴ S. Mioduszewski,³ G. C. Mishra,¹² J. T. Mitchell,³ D. P. Morrison,³ J. M. Moss,²⁶ T. V. Moukhanova,²² D. Mukhopadhyay,⁴⁹ J. Murata,^{39,37} S. Nagamiya,¹⁹ Y. Nagata,⁴⁸ J. L. Nagle,⁶ M. Naglis,⁵¹ T. Nakamura,¹³ J. Newby,²⁵ M. Nguyen,⁴⁴ B. E. Norman,²⁶ A. S. Nyanin,²² J. Nystrand,²⁸ E. O'Brien,³ C. A. Ogilvie,¹⁶ H. Ohnishi,³⁷ I. D. Ojha,⁴⁹ H. Okada,^{23,37} K. Okada,³⁸ O. O. Omiwade,¹ A. Oskarsson,²⁸ I. Otterlund,²⁸ K. Ozawa,⁵ D. Pal,⁴⁹ A. P. T. Palounek,²⁶ V. Pantuev,⁴⁴ V. Papavassiliou,³³ J. Park,⁴² W. J. Park,²¹ S. F. Pate,³³ H. Pei,¹⁶ J.-C. Peng,¹⁵ H. Pereira,⁸ V. Peresedov,¹⁷ D. Yu. Peressouko,²² C. Pinkenburg,³ R. P. Pisani,³ M. L. Purschke,³ A. K. Purwar,⁴⁴ H. Qu,¹² J. Rak,¹⁶ I. Ravinovich,⁵¹ K. F. Read,^{34,46} M. Reuter,⁴⁴ K. Reygers,²⁹ V. Riabov,³⁶ Y. Riabov,³⁶ G. Roche,²⁷ A. Romana,^{24,†} M. Rosati,¹⁶ S. S. E. Rosendahl,²⁸ P. Rosnet,²⁷ P. Rukoyatkin,¹⁷ V. L. Rykov,³⁷ S. S. Ryu,⁵² B. Sahlmueller,²⁹ N. Saito,^{23,37,38} T. Sakaguchi,^{5,50} S. Sakai,⁴⁸ V. Samsonov,³⁶ H. D. Sato,^{23,37} S. Sato,^{3,19,48} S. Sawada,¹⁹ V. Semenov,¹⁴ R. Seto,⁴ D. Sharma,⁵¹ T. K. Shea,³ I. Shein,¹⁴ T.-A. Shibata,^{37,47} K. Shigaki,¹³ M. Shimomura,⁴⁸ T. Shohjoh,⁴⁸ K. Shoji,^{23,37} A. Sickles,⁴⁴ C. L. Silva,⁴¹ D. Silvermyr,³⁴ K. S. Sim,²¹ C. P. Singh,² V. Singh,² S. Skutnik,¹⁶ W. C. Smith,¹ A. Soldatov,¹⁴ R. A. Soltz,²⁵ W. E. Sondheim,²⁶ S. P. Sorensen,⁴⁶ I. V. Sourikova,³ F. Staley,⁸ P. W. Stankus,³⁴ E. Stenlund,²⁸ M. Stepanov,³³ A. Ster,²⁰ S. P. Stoll,³ T. Sugitate,¹³ C. Suire,³⁵ J. P. Sullivan,²⁶ J. Sziklai,²⁰ T. Tabaru,³⁸ S. Takagi,⁴⁸ E. M. Takagui,⁴¹ A. Taketani,^{37,38} K. H. Tanaka,¹⁹ Y. Tanaka,³¹ K. Tanida,^{37,38} M. J. Tannenbaum,³ A. Taranenko,⁴³ P. Tarján,⁹ T. L. Thomas,³² M. Togawa,^{23,37} J. Tojo,³⁷ H. Torii,³⁷ R. S. Towell,¹ V.-N. Tram,²⁴ I. Tseruya,⁵¹ Y. Tsuchimoto,^{13,37} S. K. Tuli,² H. Tydesjö,²⁸ N. Tyurin,¹⁴ C. Vale,¹⁶ H. Valle,⁴⁹ H. W. vanHecke,²⁶ J. Velkovska,⁴⁹ R. Vertesi,⁹ A. A. Vinogradov,²² E. Vznuzdaev,³⁶ M. Wagner,^{23,37} X. R. Wang,³³ Y. Watanabe,^{37,38} J. Wessels,²⁹ S. N. White,³ N. Willis,³⁵ D. Winter,⁷ C. L. Woody,³ M. Wysocki,⁶ W. Xie,^{4,38} A. Yanovich,¹⁴ S. Yokkaichi,^{37,38} G. R. Young,³⁴ I. Younus,³² I. E. Yushmanov,²² W. A. Zajc,⁷ O. Zaudtke,²⁹ C. Zhang,⁷ J. Zimányi,^{20,†} and L. Zolin¹⁷

(PHENIX Collaboration)

¹Abilene Christian University, Abilene, Texas 79699, USA²Department of Physics, Banaras Hindu University, Varanasi 221005, India³Brookhaven National Laboratory, Upton, New York 11973-5000, USA

- ⁴University of California-Riverside, Riverside, California 92521, USA
- ⁵Center for Nuclear Study, Graduate School of Science, University of Tokyo, 7-3-1 Hongo, Bunkyo, Tokyo 113-0033, Japan
- ⁶University of Colorado, Boulder, Colorado 80309, USA
- ⁷Columbia University, New York, New York 10027, USA
and Nevis Laboratories, Irvington, New York 10533, USA
- ⁸Dapnia, CEA Saclay, F-91191, Gif-sur-Yvette, France
- ⁹Debrecen University, H-4010 Debrecen, Egyetem tér 1, Hungary
- ¹⁰ELTE, Eötvös Loránd University, H-1117 Budapest, Pázmány P. s. 1/A, Hungary
- ¹¹Florida State University, Tallahassee, Florida 32306, USA
- ¹²Georgia State University, Atlanta, Georgia 30303, USA
- ¹³Hiroshima University, Kagamiyama, Higashi-Hiroshima 739-8526, Japan
- ¹⁴IHEP Protvino, State Research Center of Russian Federation, Institute for High Energy Physics, Protvino, 142281, Russia
- ¹⁵University of Illinois at Urbana-Champaign, Urbana, Illinois 61801, USA
- ¹⁶Iowa State University, Ames, Iowa 50011, USA
- ¹⁷Joint Institute for Nuclear Research, 141980 Dubna, Moscow Region, Russia
- ¹⁸KAERI, Cyclotron Application Laboratory, Seoul, South Korea
- ¹⁹KEK, High Energy Accelerator Research Organization, Tsukuba, Ibaraki 305-0801, Japan
- ²⁰KFKI Research Institute for Particle and Nuclear Physics of the Hungarian Academy of Sciences (MTA KFKI RMKI), H-1525 Budapest 114, P.O. Box 49, Budapest, Hungary
- ²¹Korea University, Seoul, 136-701, Korea
- ²²Russian Research Center “Kurchatov Institute,” Moscow, Russia
- ²³Kyoto University, Kyoto 606-8502, Japan
- ²⁴Laboratoire Leprince-Ringuet, Ecole Polytechnique, CNRS-IN2P3, Route de Saclay, F-91128, Palaiseau, France
- ²⁵Lawrence Livermore National Laboratory, Livermore, California 94550, USA
- ²⁶Los Alamos National Laboratory, Los Alamos, New Mexico 87545, USA
- ²⁷LPC, Université Blaise Pascal, CNRS-IN2P3, Clermont-Fd, 63177 Aubiere Cedex, France
- ²⁸Department of Physics, Lund University, Box 118, SE-221 00 Lund, Sweden
- ²⁹Institut für Kernphysik, University of Muenster, D-48149 Muenster, Germany
- ³⁰Myongji University, Yongin, Kyonggido 449-728, Korea
- ³¹Nagasaki Institute of Applied Science, Nagasaki-shi, Nagasaki 851-0193, Japan
- ³²University of New Mexico, Albuquerque, New Mexico 87131, USA
- ³³New Mexico State University, Las Cruces, New Mexico 88003, USA
- ³⁴Oak Ridge National Laboratory, Oak Ridge, Tennessee 37831, USA
- ³⁵IPN-Orsay, Université Paris Sud, CNRS-IN2P3, BP1, F-91406, Orsay, France
- ³⁶PNPI, Petersburg Nuclear Physics Institute, Gatchina, Leningrad region, 188300, Russia
- ³⁷RIKEN, The Institute of Physical and Chemical Research, Wako, Saitama 351-0198, Japan
- ³⁸RIKEN BNL Research Center, Brookhaven National Laboratory, Upton, New York 11973-5000, USA
- ³⁹Physics Department, Rikkyo University, 3-34-1 Nishi-Ikebukuro, Toshima, Tokyo 171-8501, Japan
- ⁴⁰Saint Petersburg State Polytechnic University, St. Petersburg, Russia
- ⁴¹Universidade de São Paulo, Instituto de Física, Caixa Postal 66318, São Paulo CEP05315-970, Brazil
- ⁴²System Electronics Laboratory, Seoul National University, Seoul, South Korea
- ⁴³Chemistry Department, Stony Brook University, Stony Brook, SUNY, New York 11794-3400, USA
- ⁴⁴Department of Physics and Astronomy, Stony Brook University, SUNY, Stony Brook, New York 11794, USA
- ⁴⁵SUBATECH (Ecole des Mines de Nantes, CNRS-IN2P3, Université de Nantes) BP 20722-44307, Nantes, France
- ⁴⁶University of Tennessee, Knoxville, Tennessee 37996, USA
- ⁴⁷Department of Physics, Tokyo Institute of Technology, Oh-okayama, Meguro, Tokyo 152-8551, Japan
- ⁴⁸Institute of Physics, University of Tsukuba, Tsukuba, Ibaraki 305, Japan
- ⁴⁹Vanderbilt University, Nashville, Tennessee 37235, USA
- ⁵⁰Waseda University, Advanced Research Institute for Science and Engineering, 17 Kikui-cho, Shinjuku-ku, Tokyo 162-0044, Japan
- ⁵¹Weizmann Institute, Rehovot 76100, Israel
- ⁵²Yonsei University, IPAP, Seoul 120-749, Korea

(Received 14 March 2007; published 31 July 2007)

Differential elliptic flow (v_2) for ϕ mesons and (anti)deuterons ($\bar{d}d$) is measured for Au + Au collisions at $\sqrt{s_{NN}} = 200$ GeV. The v_2 for ϕ mesons follows the trend of lighter π^\pm and K^\pm mesons, suggesting that ordinary hadrons interacting with standard hadronic cross sections are not the primary driver for elliptic flow development. The v_2 values for $\bar{d}d$ suggest that elliptic flow is additive for composite particles. This further validation of the universal scaling of v_2 per constituent quark for baryons and mesons suggests that partonic collectivity dominates the transverse expansion dynamics.

An important goal of current ultrarelativistic heavy ion research is to map out the accessible regions of the quantum chromodynamics phase diagram. Central to this goal is the creation and study of a new phase of nuclear matter—the quark gluon plasma (QGP). Thermalization and deconfinement are important properties of this matter, believed to be produced in heavy ion collisions at the Relativistic Heavy Ion Collider (RHIC) [1–3].

Detailed elliptic flow measurements provide indispensable information about this high energy density matter [4–8]. Such measurements are characterized by the magnitude of the second-harmonic coefficient $v_2 = \langle e^{i2(\varphi_p - \Phi_{RP})} \rangle$, of the Fourier expansion of the azimuthal distribution of emitted particles. Here, φ_p represents the azimuthal emission angle of a particle, Φ_{RP} is the azimuthal angle of the reaction plane, and the brackets denote statistical averaging over particles and events [9,10].

At RHIC energies, there is now significant evidence that elliptic flow, in noncentral collisions, results from hydrodynamic pressure gradients developed in a locally thermalized “almond-shaped” collision zone. That is, the initial transverse coordinate-space anisotropy of this zone is converted, via particle interactions, into an azimuthal momentum-space anisotropy. Indeed, when plotted as a function of the transverse kinetic energy, $\text{KE}_T \equiv m_T - m$, divided by the number of valence quarks n_q of a given hadron ($n_q = 2$ for mesons and $n_q = 3$ for baryons), v_2/n_q shows universal scaling for a broad range of particle species [11–14] (m_T is the transverse mass). This has been interpreted as evidence that hydrodynamic expansion of the QGP occurs during a phase characterized by (i) a rather low viscosity to entropy ratio η/s [2,3,13,15,16] and (ii) independent quasiparticles which exhibit the quantum numbers of quarks [13,17–21]. A consensus on the detailed dynamical evolution of the QGP has not been reached [3,16].

Elliptic flow measurements for heavy, strange, and multistrange hadrons [22,23] can lend unique insight on reaction dynamics. Here, we use differential v_2 measurements for the ϕ meson and the deuteron to address the important question of how the existence of a hadronic phase affects v_2 : Is elliptic flow development dominantly pre- or posthadronization?

The ϕ meson is comprised of a strange (s) and an antistrange (\bar{s}) quark, and its interaction with hadrons is suppressed according to the Okubo-Zweig-Izuka (OZI) rules [24]. One consequence of this is that the ϕ meson is expected to have a rather small hadronic cross section with nonstrange hadrons (~ 9 mb) [25–27]. Such a cross section leads to a relatively large mean free path λ_ϕ , when compared to the transverse size of the emitting system. Thus, if elliptic flow was established in a phase involving hadrons interacting with their standard hadronic cross sections (posthadronization), one would expect v_2 for the ϕ meson to be significantly smaller than that for other

hadrons (e.g., p and π). A recent measurement [28] has ruled out the possibility of ϕ meson production via K^+K^- coalescence. If v_2 is established in the phase prior to hadronization, the ϕ meson provides an important benchmark test for universal scaling in that its mass is similar to that of the proton and the Λ baryon, but its v_2 should be additive with respect to the v_2 of its two constituent quarks (i.e., $n_q = 2$). This scenario also provides an important constraint for hydrodynamical models which predict a $v_2(p_T)$ ordering pattern based on the mass of different particle species. Therefore, a detailed comparison of the v_2 values for the ϕ meson with those for other particle species, comprised of the lighter u and d quarks or the heavier charm quark c , can provide unique insight on whether or not partonic collectivity plays a central role in reaction dynamics at RHIC [20,29,30].

The deuteron is a very shallow composite $p + n$ bound state, whose binding energy (~ 2.24 MeV) is much less than the hadronization temperature. Thus, it is likely that it would suffer from medium induced breakup in the hadronic phase, even if it was produced at hadronization. In fact, recent investigations [31,32] suggest that $(\bar{p}\bar{n})pn$ coalescence dominates the (anti)deuteron $(\bar{d})d$ yield in Au + Au collisions. Thus, v_2 measurements for $(\bar{d})d$ also provide an important test for the universal scaling of elliptic flow [29] in that its v_2 should be additive, first, with respect to the v_2 of its constituent hadrons and, second, with respect to the v_2 of the constituent quarks of these hadrons (i.e., $n_q = 2 \times 3$).

In the 2004 running period the PHENIX detector [33] recorded $\approx 6.5 \times 10^8$ minimum-bias events for Au + Au collisions at $\sqrt{s_{NN}} = 200$ GeV. The collision vertex z (along beam axis) was constrained to $|z| < 30$ cm of the nominal crossing point. The event centrality was determined via cuts in the space of beam-beam counter (BBC) charge versus zero degree calorimeter energy [34]. In the central rapidity region ($|\eta| \leq 0.35$) the drift chambers, each with an azimuthal coverage $\Delta\varphi = \pi/2$, and two layers of multiwire proportional chambers with pad readout (PC1 and PC3) were used for charged particle tracking and momentum reconstruction. The time-of-flight (TOF) and lead scintillator (PbSc) detectors were used for charged particle identification [6,7].

Time-of-flight measurements from the TOF and PbSc were used in conjunction with the measured momentum and flight-path length to generate a mass-squared (m^2) distribution [35]. A track confirmation hit within a 2.5σ matching window in PC3 or TOF/PbSc served to eliminate most albedo, conversions, and resonance decays. A momentum dependent $\pm 2\sigma$ cut about each peak in the m^2 distribution was used to identify pions (π^\pm), kaons (K^\pm), (anti)protons [$(\bar{p})p$], and (anti)deuterons [$(\bar{d})d$] in the range $0.2 < p_T < 2.5$ GeV/ c , $0.3 < p_T < 2.5$ GeV/ c , $0.5 < p_T < 4.5$ GeV/ c , and $1.1 < p_T < 4.5$ GeV/ c , respectively, in the TOF, and to identify K^\pm in the range

$0.3 < p_T < 1.5$ GeV/ c in the PbSc. This gave $\sim 59\,000 \bar{d} + d$. An invariant mass analysis of the $\phi \rightarrow K^+ K^-$ decay channel yielded $\sim 340\,000 \phi$ mesons with relatively good signal to background (14%–42% for the mass window $|m_{\text{inv}}| = 5$ MeV/ c^2 about the ϕ meson peak) over the range $1.0 < p_T < 5.5$ GeV/ c for $K^+ K^-$ pairs.

The reaction plane method [6] was used to correlate the azimuthal angles of charged tracks with the azimuth of the event plane Φ_2 , determined via hits in the two BBCs covering the pseudorapidity range $3.0 < |\eta| < 3.9$. The large pseudorapidity gap $\Delta\eta > 2.75$ between the central arms and the particles used for reaction plane determination reduces the influence of possible nonflow contributions, especially those from dijets [36]. Charge averaged values of $v_2 = \langle \cos(2(\varphi_p - \Phi_2)) \rangle / \langle \cos(2(\Phi_2 - \Phi_{\text{RP}})) \rangle$ were evaluated for π^\pm , K^\pm , $(\bar{p})p$, and $(\bar{d})d$. Here, the denominator represents a resolution factor to correct for the difference between the estimated Φ_2 and the true azimuth Φ_{RP} of the reaction plane [6,37]. The estimated resolution factor of the combined reaction plane from both BBCs has an average of 0.33 over centrality, with a maximum of about 0.42 in midcentral collisions [6,12]. The associated systematic error is estimated to be $\sim 5\%$ for π^\pm , K^\pm , and $(\bar{p})p$. A p_T dependent correction factor ($\sim 5\%$ – 11%) was applied to the v_2 values for $(\bar{d})d$, to account for background contributions to the (anti)deuteron peak (signal) in the m^2 distributions (dash-dotted curve in Fig. 1(a)):

$$v_2^{(\bar{d})d}(p_T) = [v_2^{s+bg}(p_T) - (1 - R)v_2^{bg}(p_T)]/R, \quad (1)$$

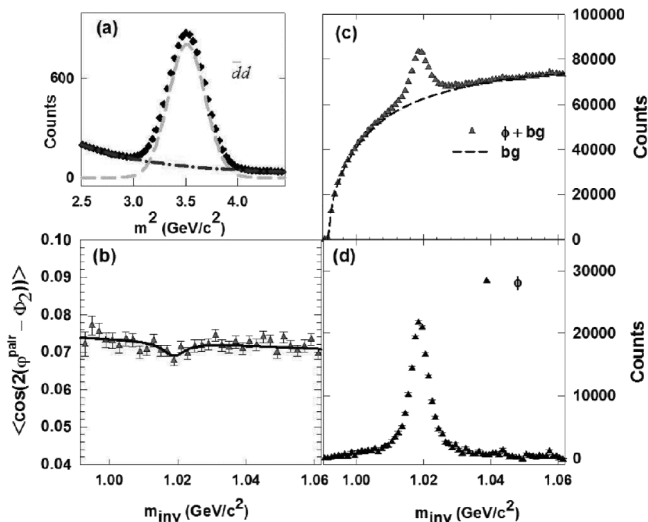


FIG. 1. (a) m^2 distribution for \bar{d}, d for $p_T = 1.6\text{--}2.9$ GeV/ c , (b) $\langle \cos(2(\varphi^{\text{pair}} - \Phi_2)) \rangle$ versus m_{inv} ; the solid line is a fit to the data with Eq. (2). (c) m_{inv} distributions for foreground (points) and background (dashed line) $K^+ K^-$ pairs ($p_T^{\text{pair}} = 1.6\text{--}2.7$ GeV/ c) for 20%–60% central Au + Au collisions. (d) m_{inv} distribution after subtraction of the background.

where $v_2^{s+bg}(p_T)$ is the measured v_2 for $(\bar{d})d +$ background at a given p_T , R is the ratio signal/(signal + background) at that p_T , and $v_2^{bg}(p_T)$ is the elliptic flow of the background evaluated for m^2 values outside of the $(\bar{d})d$ peaks.

Extraction of the elliptic flow values for the ϕ meson (v_2^ϕ) followed the invariant mass (m_{inv}) method [38]. For each event, m_{inv} , p_T^{pair} , and φ^{pair} for each $K^+ K^-$ pair were evaluated. Then, for each p_T^{pair} bin, $v_2^{\text{pair}} = \langle \cos(2(\varphi^{\text{pair}} - \Phi_2)) \rangle$ was evaluated as a function of m_{inv} as shown in Fig. 1(b). The value $v_2^\phi(p_T)$ was then obtained from $v_2^{\text{pair}}(m_{\text{inv}})$ via an expression similar to Eq. (1):

$$v_2^{\text{pair}}(m_{\text{inv}}) = v_2^\phi R(m_{\text{inv}}) + v_2^{\text{bg}}(m_{\text{inv}})[1 - R(m_{\text{inv}})], \quad (2)$$

where $R(m_{\text{inv}}) = N_\phi(m_{\text{inv}})/[N_\phi(m_{\text{inv}}) + N_{\text{bg}}(m_{\text{inv}})]$ and $N_\phi(m_{\text{inv}})$ and $N_{\text{bg}}(m_{\text{inv}})$ are distributions for the ϕ meson and the combinatoric background, respectively, $N_\phi(m_{\text{inv}})$ is obtained from the distribution $N_{\text{pair}}(m_{\text{inv}})$ of $K^+ K^-$ pairs from the same event (foreground); $N_{\text{bg}}(m_{\text{inv}})$ is the distribution of pairs obtained from different events with similar centrality, vertex, and event plane orientation [39]. Figure 1(c) shows a representative example of the latter distributions for $1.6 \leq p_T^{\text{pair}} \leq 2.7$ GeV/ c and reaction centrality 20%–60%. A clear peak signaling the ϕ meson is apparent in the foreground distribution for $m_{\text{inv}} \sim 1.02$ GeV/ c^2 . The background distribution was normalized to that for the foreground in the region $1.04 < m_{\text{inv}} < 1.2$ GeV/ c^2 and subtracted to obtain the $N_\phi(m_{\text{inv}})$ distribution shown in Fig. 1(d); a relatively narrow ϕ meson peak is apparent.

Determination of the ratio $R(m_{\text{inv}})$ was facilitated by fitting this distribution with a Breit-Wigner function plus a linear function, as shown by the solid curve in Fig. 1(c). To ensure robust v_2^ϕ extraction, the combinatorial background was constructed such that $v_2^{\text{bg}}(m_{\text{inv}})$ gave the same value as $v_2^{\text{pair}}(m_{\text{inv}})$ for m_{inv} values not associated

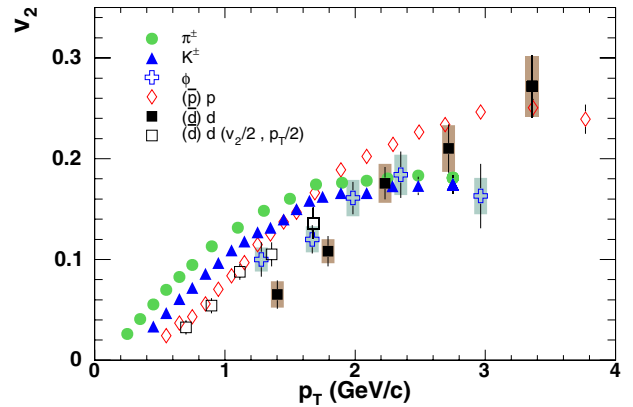


FIG. 2 (color online). Comparison of differential $v_2(p_T)$ for ϕ mesons, $(\bar{d})d$, π^\pm , K^\pm , and $(\bar{p})p$ (as indicated). Results are shown for 20%–60% central Au + Au collisions.

with the ϕ meson peak. Values for v_2^ϕ were extracted via direct fits to the $v_2^{\text{pair}}(m_{\text{inv}})$ distribution for each p_T^{pair} selection [cf. Eq. (2)]. That is, $v_2^{\text{bg}}(m_{\text{inv}})$ was parametrized as a linear or quadratic function of m_{inv} (depending on the p_T^{pair} bin) and v_2^ϕ was taken as a fit parameter.

The accuracy of the extraction procedure was verified by checking that the m_{inv} dependence of the sine coefficients, $v_{s,2}^{\text{pair}}(m_{\text{inv}}) = \langle \sin(2(\varphi^{\text{pair}} - \Phi_2)) \rangle$, were all zero within statistical errors. An alternative ‘‘subtraction method’’ [40,41], in which the raw ϕ meson yield distribution $dN/d(\varphi_\phi - \Phi_2)$ was extracted and fitted with the function $N\{1 + 2v_2^\phi \cos[2(\varphi_\phi - \Phi_2)]\}$, also showed good agreement, albeit with larger error bars; N is an arbitrary normalization constant.

The differential $v_2(p_T)$ obtained for $(\bar{d})d$ and the ϕ meson, for centrality 20%–60%, are compared to those for π^\pm , K^\pm , and $(\bar{p})p$ in Fig. 2. This centrality selection was so chosen to (i) maximize the ϕ meson signal to background ratio over the full range of p_T bins and (ii) enhance the distinction between baryon and meson v_2 in the intermediate p_T range. The shaded bands for $(\bar{d})d$ and the ϕ meson indicate systematic errors ($\sim 6\%$ – 15%), primarily associated with the determination of R and $R(m_{\text{inv}})$, v_2^{bg} and $v_2^{\text{bg}}(m_{\text{inv}})$ [cf. Eqs. (1) and (2)], and fitting.

The values for $v_2^{(\bar{d})d}$ shown in Fig. 2 are as much as a factor ≈ 2.5 lower than those for π^\pm at low p_T . This mass ordering pattern reflects the detailed expansion dynamics of the created matter. As a first test of whether or not v_2 for $(\bar{d})d$ is additive with respect to its constituent hadrons, $v_2^{(\bar{d})d}/2$ versus $p_T/2$ is compared to $v_2^{(\bar{p})p}$ versus p_T . Within errors, they show good agreement as would be expected if $v_2^{(\bar{d})d}$ is additive. The large magnitude of v_2 for the ϕ meson gives an initial indication that significant flow development occurs prior to hadronization.

The left and right panels of Fig. 3 compare the unscaled and scaled results (respectively) for v_2 versus KE_T for π^\pm , K^\pm , $(\bar{p})p$, $(\bar{d})d$, and the ϕ meson, in 20%–60% central Au + Au collisions. The left panel clearly shows that, despite its mass which is comparable to that for the proton, $v_2(\text{KE}_T)$ for the ϕ meson follows the flow pattern of the other lighter mesons (π and K), whose cross sections are not OZI suppressed. A similar pattern is also observed for the $v_2(\text{KE}_T)$ values inferred for D mesons (comprised of charmed quarks) from nonphotonic electron measurements [13,23,42]. These observations indicate that, when elliptic flow develops, the constituents of the flowing medium are not ordinary hadrons interacting with their standard hadronic cross sections. Instead, partonic collectivity appears to dominate the transverse expansion dynamics of light, strange, and charmed quarks via a common velocity field.

Interestingly, the $v_2(\text{KE}_T)$ results shown for the $(\bar{d})d$ and the ϕ meson are essentially identical at low KE_T ($\text{KE}_T \lesssim 1$ GeV), and are in good agreement with those for other

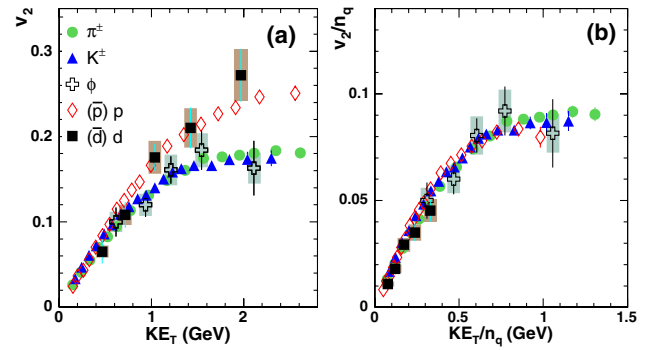


FIG. 3 (color online). (a) v_2 vs KE_T for several identified particle species obtained in midcentral (20%–60%) Au + Au collisions. (b) v_2/n_q vs KE_T/n_q for the same particle species shown in (a). The shaded bands indicate systematic error estimates for $(\bar{d})d$ and ϕ mesons (see text).

charged hadrons, including the pion with a mass ~ 13 times smaller than the deuteron. This strengthens the earlier finding that, for low KE_T , all particle species exhibit the same v_2 irrespective of their mass [11–13]. The expected difference between $(\bar{d})d$ and $(\bar{p})p$ for $\text{KE}_T \gtrsim 1$ GeV is not tested in Fig. 3, due to the limited KE_T range of the $(\bar{d})d$ data.

The right panel of Fig. 3 shows the results for a validation test of universal scaling for $v_2(\text{KE}_T)$ of baryons and mesons [11–13]. The value $n_q = 2 \times 3$ is used for $(\bar{d})d$ to account for its composite ($p + n$) nature. The scaled results shown in Fig. 3(b) clearly serve as further validation for the experimentally observed universal scaling of v_2 for baryons and mesons [11–13]. This finding lends strong support to the notion that the high energy density matter, created in RHIC collisions, comprise a prehadronization state that contains the prerequisite quantum numbers of the hadrons to be formed. Thus, it appears that partonic collectivity dominates the expansion dynamics of these collisions. The special role of KE_T as a scaling variable is not fully understood.

We have presented differential v_2 measurements for the ϕ meson and deuteron. For a broad range of KE_T values, the differential $v_2(\text{KE}_T)$ for the ϕ meson follows the flow pattern for other light mesons whose cross sections are not OZI suppressed. The composites $(\bar{d})d$ follow the flow pattern for baryons with additive v_2 values. When v_2/n_q is plotted as a function of the transverse kinetic energy scaled by the number of valence quarks (i.e., KE_T/n_q), universal scaling results for all particle species measured. These observations suggest that the transverse expansion dynamics leading to elliptic flow development cannot be understood in terms of ordinary hadrons interacting with their standard hadronic cross sections, but rather in terms of a prehadronization state in which the flowing medium reflects quark degrees of freedom.

We thank the staff of the Collider-Accelerator and Physics Departments at BNL for their vital contributions. We acknowledge support from the Office of NP in DOE Office of Science and NSF (U.S.A.), MEXT and JSPS (Japan), CNPq and FAPESP (Brazil), NSFC (China), IN2P3/CNRS, and CEA (France), BMBF, DAAD, and AvH (Germany), OTKA (Hungary), DAE (India), ISF (Israel), KRF and KOSEF (Korea), MES, RAS, and FAAE (Russia), VR and KAW (Sweden), U.S. CRDF for the FSU, US-Hungarian NSF-OTKA-MTA, and U.S.-Israel BSF.

*PHENIX Spokesperson.

jacak@skipper.physics.sunysb.edu

†Deceased.

- [1] K. Adcox *et al.*, Nucl. Phys. **A757**, 184 (2005).
 [2] M. Gyulassy and L. McLerran, Nucl. Phys. **A750**, 30 (2005).
 [3] E. V. Shuryak, Nucl. Phys. **A750**, 64 (2005).
 [4] K. H. Ackermann *et al.*, Phys. Rev. Lett. **86**, 402 (2001).
 [5] K. Adcox *et al.*, Phys. Rev. Lett. **89**, 212301 (2002).
 [6] S. S. Adler *et al.*, Phys. Rev. Lett. **91**, 182301 (2003).
 [7] S. S. Adler *et al.*, Phys. Rev. Lett. **94**, 232302 (2005).
 [8] R. A. Lacey, Nucl. Phys. **A774**, 199 (2006).
 [9] M. Demoulin *et al.*, Phys. Lett. B **241**, 476 (1990).
 [10] S. Voloshin and Y. Zhang, Z. Phys. C **70**, 665 (1996).
 [11] M. Issah and A. Taranenko, arXiv:nucl-ex/0604011.
 [12] A. Adare *et al.*, Phys. Rev. Lett. **98**, 162301 (2007).
 [13] R. A. Lacey and A. Taranenko, arXiv:nucl-ex/0610029.
 [14] J. Jia and C. Zhang, Phys. Rev. C **75**, 031901(R) (2007).
 [15] U. W. Heinz and P. F. Kolb, Nucl. Phys. **A702**, 269 (2002).
 [16] M. Asakawa, S. A. Bass, and B. Muller, Phys. Rev. Lett. **96**, 252301 (2006).
 [17] S. A. Voloshin, Nucl. Phys. **A715**, 379 (2003).
 [18] R. J. Fries, B. Muller, C. Nonaka, and S. A. Bass, Phys. Rev. C **68**, 044902 (2003).
 [19] V. Greco, C. M. Ko, and P. Levai, Phys. Rev. C **68**, 034904 (2003).
 [20] N. Xu, Nucl. Phys. **A751**, 109 (2005).
 [21] B. Müller and J. L. Nagle, Annu. Rev. Nucl. Part. Sci. **56**, 93 (2006).
 [22] M. Oldenburg, J. Phys. G **32**, S563 (2006).
 [23] A. Adare *et al.*, Phys. Rev. Lett. **98**, 172301 (2007).
 [24] S. Okubo, Phys. Lett. **5**, 165 (1963).
 [25] A. Shor, Phys. Rev. Lett. **54**, 1122 (1985).
 [26] C. M. Ko and D. Seibert, Phys. Rev. C **49**, 2198 (1994).
 [27] K. Haglin, Nucl. Phys. **A584**, 719 (1995).
 [28] J. Adams *et al.* (STAR Collaboration), Phys. Lett. B **612**, 181 (2005).
 [29] C. Nonaka *et al.*, Phys. Rev. C **69**, 031902 (2004).
 [30] J. H. Chen *et al.*, Phys. Rev. C **74**, 064902 (2006).
 [31] C. Adler *et al.*, Phys. Rev. Lett. **87**, 262301 (2001).
 [32] S. S. Adler *et al.*, Phys. Rev. Lett. **94**, 122302 (2005).
 [33] K. Adcox *et al.*, Nucl. Instrum. Methods Phys. Res., Sect. A **499**, 469 (2003).
 [34] K. Adcox *et al.*, Phys. Rev. C **69**, 024904 (2004).
 [35] S. S. Adler *et al.*, Phys. Rev. C **69**, 034909 (2004).
 [36] J. Jia (PHENIX Collaboration), Nucl. Phys. **A783**, 501 (2007).
 [37] A. M. Poskanzer and S. A. Voloshin, Phys. Rev. C **58**, 1671 (1998).
 [38] N. Borghini and J. Y. Ollitrault, Phys. Rev. C **70**, 064905 (2004).
 [39] S. S. Adler *et al.*, Phys. Rev. C **72**, 014903 (2005).
 [40] D. Pal, Nucl. Phys. **A774**, 489 (2006).
 [41] S. S. Adler *et al.*, Phys. Rev. Lett. **96**, 032302 (2006).
 [42] V. Greco, C. M. Ko, and R. Rapp, Phys. Lett. B **595**, 202 (2004).